



---

# Audio Engineering Society Convention Paper

Presented at the 128th Convention  
2010 May 22–25 London, UK

*The papers at this Convention have been selected on the basis of a submitted abstract and extended precis that have been peer reviewed by at least two qualified anonymous reviewers. This convention paper has been reproduced from the author's advance manuscript, without editing, corrections, or consideration by the Review Board. The AES takes no responsibility for the contents. Additional papers may be obtained by sending request and remittance to Audio Engineering Society, 60 East 42<sup>nd</sup> Street, New York, New York 10165-2520, USA; also see [www.aes.org](http://www.aes.org). All rights reserved. Reproduction of this paper, or any portion thereof, is not permitted without direct permission from the Journal of the Audio Engineering Society.*

---

## Sound Field Recording by Measuring Gradients

Mihailo Kolundžija<sup>1</sup>, Christof Faller<sup>1</sup>, and Martin Vetterli<sup>1,2</sup>

<sup>1</sup>*Audiovisual Communications Laboratory, Ecole Polytechnique Fédérale de Lausanne, 1015 Lausanne, Switzerland*

<sup>2</sup>*Department of EECS, University of California at Berkeley, Berkeley CA 94720, USA*

Correspondence should be addressed to Mihailo Kolundžija ([mihailo.kolundzija@epfl.ch](mailto:mihailo.kolundzija@epfl.ch))

### ABSTRACT

Gradient based microphone arrays, the horizontal sound field's plane wave decomposition, and the corresponding circular harmonics decomposition are reviewed. Further, a general relation between directivity patterns of the horizontal sound field gradients and the circular harmonics of any order is derived. Based on this relation, a number of example differential microphone arrays are analyzed, including arrays capable of approximating the sound pressure gradients necessary for obtaining the circular harmonics up to order three.

### 1. INTRODUCTION

Directional microphones have an appealing property of responding differently to sounds arriving from different directions, characterized by their directivity pattern<sup>1</sup>  $e(\theta)$  in two and  $e(\theta, \phi)$  in three dimensions. Based on their working principle, directional microphones can be classified into two categories: wave type and gradient type [1–3]. Since the wave type microphones are not practical for dimensional constraints (microphone size comparable to the wavelength of the measured waves), they are not widely used and are not the topic of this paper. The fo-

cus will be on the more widely used gradient type. Gradient microphones, in a general sense, have a directional response which is dependent on the sound pressure difference between points spaced at a distance that is small compared to the wavelength [1–3]. Similarly to gradient microphones, differential microphone arrays, which combine delayed sound pressure signals from two or more closely-spaced microphones, are also classified as directional.

Directional microphones can be used for noise and interference reduction, which are desirable in telephony, teleconferencing, and sound recording. Another important application is sound capture for stereo and multichannel surround systems. The

---

<sup>1</sup>The directivity pattern of a directional microphone is usually frequency-dependent.

sound capture is done in a way that the microphones' polar characteristics—or the encoding functions [4]—encode the source location to level differences relating to virtual source localization during playback.

The first spatial sound recording techniques involving directional microphones, such as MS and XY stereo coding invented by Blumlein [5], became too restricting for the use with more complex surround sound systems. One such system, Ambisonics [6–8], relies on high-order components of the sound field in order to enable extended listening area reproduction. Such paradigm resulted in the concept of *sound field microphone*—a system that captures circular or spherical harmonic components of the sound field in one point.

First sound field microphones appeared in the 70's (e.g., see [7,9]), and are still widely used today. They deliver the so-called first-order B-format signal set, which consists of a sound pressure signal, denoted as  $W$ , and three first-order sound field spherical harmonic components, denoted as  $X$ ,  $Y$  and  $Z$ . Despite of the improvements it brought to the spatial sound recording practice, the works of Bamford *et al.* [10] and Daniel [11] have shown that for accurate sound field reproduction over a wide listening area, first-order ambisonic recording was insufficient. The last decade has seen many designs of planar and three-dimensional sound field microphones built using circular (e.g., see [12]) or spherical (e.g., see [13–16]) microphone arrays, respectively. This paper's focus is on the planar case.

The contributions of this paper are:

- It is shown that by measuring a sound field's gradients one can obtain its circular harmonic coefficients.
- It is shown how horizontal sound field microphones up to order three can be built as small arrays of pressure and/or gradient microphones which measure the sound field gradients needed for obtaining its circular harmonic coefficients.

The paper is organized as follows. Section 2 reviews the plane wave decomposition and circular harmonic representation of the horizontal sound field. Section 3 reviews the theory of gradient and differential

microphones and arrays. The correspondence between a plane-wave sound field's circular harmonics and directivity pattern of its gradients is shown in Section 4. Section 5 proposes practical microphone configurations for measuring gradients and computing the horizontal sound field's circular harmonic coefficients of orders two and three. Section 6 presents results of simulation experiments of the second-order horizontal sound field microphone proposed in Section 5. The conclusions are in Section 7.

## 2. SOUND FIELD DECOMPOSITION

### 2.1. Plane wave representation

Plane waves are solutions to the wave equation of the form [12, 17]

$$p(\mathbf{r}, t) = Ae^{j(\omega t + \mathbf{k} \cdot \mathbf{r})}, \quad (1)$$

where  $A$  is the complex amplitude<sup>2</sup> (conveying the information about both the real amplitude and the initial phase),  $\omega$  is the temporal frequency and  $\mathbf{k}$  is the wave vector pointing toward the direction of sound arrival, having the intensity  $k = \frac{\omega}{c}$ , where  $c$  is the speed of sound.

A distribution of the sound pressure in space and time,  $p(\mathbf{r}, t)$ , can be represented as a sum of plane- and evanescent waves [17]. If the sound sources are far away from the region of interest, the non-propagating evanescent wave contributions can be neglected. As most of the literature on surround sound systems, this paper considers only the sound fields emanating from sources which are sufficiently far, such that in the region of interest their wavefront can be considered as flat and without amplitude decay. In other words, the considered sound fields are composed of plane waves.

As most spatial sound systems are two-dimensional, the analysis of the sound field in this paper focuses on the horizontal plane ( $z = 0$ ), implicitly assuming that plane waves propagate parallel to the horizontal plane.

<sup>2</sup>This paper uses the widely-used theoretical analysis of an analytic (complex-valued) sound pressure field. The physical sound pressure, which is a real-valued function of space and time, can be obtained from the real part of its analytic counterpart.

## 2.2. Circular harmonic representation

A sound field emanating from far-field sources can completely be characterized by the *frequency-dependent source distribution*  $S(k, \theta)$ , or its time Fourier transform pair, *angular source distribution*  $s(t, \theta)$  [12]. Moreover, since  $s(t, \theta)$  is a  $2\pi$ -periodic function of angle  $\theta$ , it can be represented through its Fourier series expansion

$$s(t, \theta) = a_0(t) + \sum_{n=1}^{\infty} a_n(t) \cos(n\theta) + \sum_{n=1}^{\infty} b_n(t) \sin(n\theta), \quad (2)$$

where the Fourier coefficients  $a_n(t)$  and  $b_n(t)$  are given by

$$\begin{aligned} a_n(t) &= \epsilon_n \frac{1}{\pi} \int_0^{2\pi} s(t, \theta) \cos(n\theta) d\theta \\ b_n(t) &= \frac{1}{\pi} \int_0^{2\pi} s(t, \theta) \sin(n\theta) d\theta, \end{aligned} \quad (3)$$

with

$$\epsilon_n = \begin{cases} \frac{1}{2}, & n = 0 \\ 1, & n > 0 \end{cases}. \quad (4)$$

In the following, the periodic functions  $\cos(n\theta)$  and  $\sin(n\theta)$  are referred to as *circular harmonics*, and the Fourier coefficients  $a_n(t)$  and  $b_n(t)$  as *circular harmonic coefficients*.

The circular harmonic coefficients are an equivalent representation of the sound pressure field composed of plane waves.

## 2.3. Measuring circular harmonic coefficients

The signal captured with an ideal directional microphone with directivity pattern  $\epsilon(\theta)$  can be expressed as

$$m(t) = \int_0^{2\pi} \epsilon(\theta) s(t, \theta) d\theta. \quad (5)$$

The signal  $m(t)$  resembles the circular harmonic coefficients  $a_n(t)$  and  $b_n(t)$  of the angular source distribution's Fourier series expansion from (3), and gives a way to indirectly capture the sound pressure field in a region of interest. Namely, to record the circular harmonic coefficients  $a_n(t)$  and  $b_n(t)$ —which completely specify the sound pressure field  $p(\mathbf{r}, t)$  in the source-free area around the measurement point—it suffices to use a set of coincident directional microphones whose directional responses are

equal to the circular harmonics:  $e_{a_n}(\theta) = \cos(n\theta)$  and  $e_{b_n}(\theta) = \sin(n\theta)$ , with  $n \geq 0$ .

## 3. ANALYSIS OF GRADIENT AND DIFFERENTIAL MICROPHONES AND ARRAYS

### 3.1. Gradient microphones

Gradient microphones are acousto-electrical transducers which were introduced by Olson (e.g., see [1, 2]) more than 50 years ago. Conceptually, gradient microphones were conceived as devices whose output is proportional to components of the gradient or spatial derivatives of the sound pressure field. Cotterell gave a theoretical overview of gradient microphones in [18], describing them as devices that measure projections of the sound pressure field's gradient onto a vector  $\mathbf{u}$  defined by the microphone's axis. Assuming the sound pressure field is composed of a plane wave

$$p(\mathbf{r}, t) = A e^{j(\omega t + \mathbf{k} \cdot \mathbf{r})}, \quad (6)$$

where  $\omega$  is the angular frequency and  $\mathbf{k}$  is the wave vector, the response of an ideal gradient microphone of order  $n$  is given by [18, 19]

$$D_{\mathbf{u}}^n p(\mathbf{r}, t) = (jk)^n (\cos \theta)^n p(\mathbf{r}, t), \quad (7)$$

where  $\theta$  is the incidence angle of the plane wave arrival direction relative to the microphone's axis, e.g. the angle between vectors  $\mathbf{k}$  and  $\mathbf{u}$ .

It is also worth noting that the first-order, bidirectional gradient microphone is referred to as a *velocity microphone*, as the time-integration of the signal on the right side of (7), for  $n = 1$ , is equal to the projection of the particle velocity vector onto the vector  $\mathbf{u}$  [18].

Important aspects of gradient microphones, considered in the following, are:

- Their directivity pattern is proportional to  $(\cos \theta)^n$ , where  $n$  is the microphone's order.
- Their frequency characteristic is of the form  $(jk)^n$ , where  $k$  is the wave number, requiring compensation by  $n$  ideal time-integrators.

### 3.2. Practical gradient microphones

Practical gradient microphones are based on the principle of finite-difference approximation of sound

pressure field's derivatives. They combine values of the sound pressure field in multiple, closely-spaced points,<sup>3</sup> either acoustically (pressure at two faces of a diaphragm) or electronically (pressure at different microphones of a microphone array).

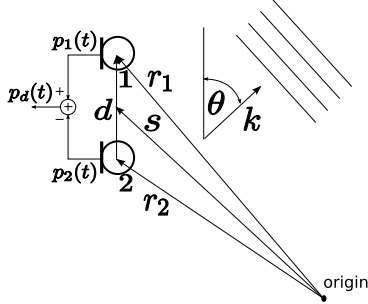


**Fig. 1:** First-order gradient microphone realization using two pressure-sensing elements.

The simplest and the most widely used [19] gradient microphone is the first-order gradient microphone (also called *dipole* and *velocity microphone*) with bidirectional, figure-of-eight directivity pattern. As previously mentioned, it is based on taking a difference in sound pressure between two closely-spaced points, an illustration of which is shown in Fig. 1. For a single plane wave, the first-order gradient microphone's response has the form [20]:

$$\begin{aligned} g^{(1)}(\mathbf{r}, t) &= p_1(t) - p_2(t) \\ &= 2j \sin\left(\frac{kd}{2} \cos\theta\right) p(\mathbf{r}, t), \end{aligned} \quad (8)$$

where  $\theta$  is the angle between the vector  $\mathbf{d}$  ( $\mathbf{d} = \mathbf{r}_1 - \mathbf{r}_2$ ) and the wave vector  $\mathbf{k}$ .

Generalizing to the gradient microphone of order  $n$ , which takes a finite-difference derivative approximation using  $n + 1$  pressure microphones spaced at distance  $d$ , the following response to a plane-wave sound field is obtained:

$$g^{(n)}(\mathbf{r}, t) = (2j)^n \left(\sin\left(\frac{kd}{2} \cos\theta\right)\right)^n p(\mathbf{r}, t), \quad (9)$$

where  $\theta$  is the incident angle as in (8).

Fig. 2 shows directivity patterns of first- and third-order practical gradient microphones for different ratios between the inter-microphone distance  $d$  and the wavelength  $\lambda$ .

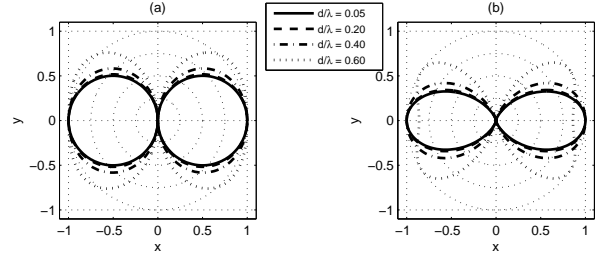


**Fig. 2:** First- (a) and third-order (b) gradient microphone directivity patterns in plane-wave sound field for different ratios  $d/\lambda$  between the inter-microphone distance  $d$  and plane wave's wavelength  $\lambda$ .

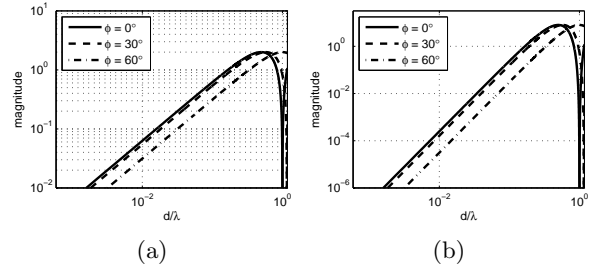


**Fig. 3:** First- (a) and third-order (b) gradient microphone frequency characteristics in plane-wave sound field at different wave incidence angles.

When the expression  $\frac{kd}{2} \cos\theta$  in the argument of the sine function in (9) is small,  $\sin x$  can be approximated by  $x$ , and the response of a practical gradient microphone, given in (9), becomes proportional to the response of an ideal gradient microphone given in (7). As can be seen in Fig. 2, due to aliasing, the directivity pattern noticeably deviates from the desired one at wavelengths  $\lambda \approx 3d$  or shorter.

Important properties of practical gradient microphones that are considered later in this paper are:

- Their working frequency range is limited by the used inter-microphone distance  $d$ .
- Their frequency-characteristic in the working frequency range is high-pass and proportional to  $\omega^n$ , requiring a low-pass compensation at the output.

<sup>3</sup>Points are spaced at a distance much shorter than the wavelength.

- Their directivity pattern in the working frequency range is bidirectional, proportional to  $(\cos \theta)^n$ , where  $\theta$  is the sound wave incident angle.

### 3.3. Differential microphone arrays

The idea of taking finite-difference approximations of the sound pressure field's spatial derivatives resulting in bidirectional directivity pattern was generalized by Olson (e.g. see [1]). He presented the concept of unidirectional microphones, built as linear combinations of gradient microphones of different orders,<sup>4</sup> whose directivity pattern has the form

$$e(\theta) = \sum_{i=0}^n a_n(\cos \theta)^i. \quad (10)$$

A typical example of a unidirectional microphone is the cardioid microphone, which is the mostly used directional microphone today [19]. The cardioid microphone contains equal contributions from pressure and first-order gradient microphones, and its directivity pattern is given by

$$e(\theta) = \frac{1}{2}(1 + \cos \theta). \quad (11)$$

Furthermore, Olson presented in [1] a way of achieving the effects of combining gradient microphones of different orders by combining gradient microphones' signals with delay elements and appropriate scaling. Recently, Elko popularized these microphone arrays under the name *differential microphone arrays* and *superdirectional microphones* (e.g. see [19, 21]). Under such classification, gradient microphones are only a special case of differential microphones. Recently, the authors showed in [22] that both gradient and differential microphone arrays can be unified using spatio-temporal gradient analysis of the sound field.

## 4. SOUND FIELD MEASUREMENT WITH GRADIENT MICROPHONES

The sound field emanating from far-field sources can be described by the angular source distribution  $s(t, \theta)$  or the circular harmonic coefficients  $a_n(t)$  and  $b_n(t)$ , as pointed out in Section 2. Consequently, the

<sup>4</sup>The pressure microphone is considered a gradient microphone of order zero.

sound field composed of plane waves can be completely captured with a set of coincident directional microphones whose directivity patterns are proportional to circular harmonics  $\cos(n\theta)$  and  $\sin(n\theta)$ . However, one can use a set of coincident directional microphones with different directivity patterns, as long as they provide a representation equivalent to the one based on circular harmonics. In the following, it will be shown that gradient microphones represent such a set.

For gradient microphones of orders zero and one, the directivity patterns are equal (and hence equivalent) to the circular harmonics of orders zero and one. For orders higher than one, one can use the identity defining the Chebyshev polynomials of the first kind,

$$T_n(\cos \theta) = \cos(n\theta), \quad (12)$$

for obtaining the representation of circular harmonics in terms of gradient microphones' directivity patterns  $(\cos \theta)^m$ . These results are stated in the following two propositions:

**Proposition 1.** *The directivity pattern of the form  $\cos(n\theta)$  can be obtained as a linear combination of directivity patterns  $(\cos \theta)^m$  of different orders  $m$ , where  $m \leq n$ .*

*Proof.* The proof follows directly from the definition of the Chebyshev polynomial of the first kind, given in (12).  $\square$

**Proposition 2.** *The directivity pattern of the form  $\sin(n\theta)$  can be obtained as a linear combination of the directivity patterns  $(\cos(\theta - \frac{\pi}{2n}))^m$  or  $(\cos(\theta + \frac{3\pi}{2n}))^m$  of different orders  $m$ , where  $m \leq n$ .*

*Proof.* Using the identity

$$\sin \theta = \cos\left(\theta - \frac{\pi}{2}\right), \quad (13)$$

$\sin(n\theta)$  can be expressed as a cosine:

$$\begin{aligned} \sin(n\theta) &= \cos\left(n\theta - \frac{\pi}{2}\right) \\ &= \cos\left(n\left(\theta - \frac{\pi}{2n}\right)\right). \end{aligned} \quad (14)$$

Equivalently,  $\sin(n\theta)$  can be expressed as:

$$\begin{aligned} \sin(n\theta) &= \cos\left(n\theta + \frac{3\pi}{2}\right) \\ &= \cos\left(n\left(\theta + \frac{3\pi}{2n}\right)\right). \end{aligned} \quad (15)$$

Applying Proposition 1 to the right side of (14) or (15) for the angle  $(\theta - \frac{\pi}{2n})$  or  $(\theta + \frac{3\pi}{2n})$ , respectively, gives

$$\sin(n\theta) = T_n(\cos(\theta - \frac{\pi}{2n})) \quad (16)$$

$$\sin(n\theta) = T_n(\cos(\theta + \frac{3\pi}{2n})), \quad (17)$$

which completes the proof.  $\square$

It should be noted that  $(\cos(\theta - \frac{\pi}{2n}))^m$  and  $(\cos(\theta + \frac{3\pi}{2n}))^m$  are directivity patterns of gradient microphones of order  $m$ , whose main axis is not along the axis  $x$ , but is rotated relative to it by angles  $\frac{\pi}{2n}$  and  $-\frac{3\pi}{2n}$ , respectively.

It should now be clear how the circular harmonic coefficients  $a_n(t)$  and  $b_n(t)$  can be obtained by the use of gradient microphones:

- The circular harmonic coefficient  $a_n(t)$  can be obtained by linearly combining the outputs of gradient microphones of orders up to and including  $n$ , whose axes lie along the axis  $x$ . The contribution of each gradient microphone is obtained from the definition of the Chebyshev polynomial of the first kind, given in (12).
- The circular harmonic coefficient  $b_n(t)$  can be obtained by linearly combining the outputs of gradient microphones of orders up to and including  $n$ , whose axes lie along the line that goes through the origin (microphone's center) and forms the angle  $\frac{\pi}{2n}$  or the angle  $\frac{3\pi}{2n}$  with the axis  $x$ ; the contribution of each gradient microphone is obtained by applying the expression (16) or (17), respectively.

## 5. PRACTICAL, GRADIENT-BASED SOUND FIELD MICROPHONES

The sound field decomposition approach used in this paper is based on the result from Section 4, where it was shown how a full decomposition of the horizontal sound field, evoked by sources in the far field, can be achieved by coincidentally measuring its gradients of different orders along different directions. Namely, using the results of Propositions 1 and 2 from Section 4, one can measure circular harmonic coefficients of the horizontal sound field by combining gradient microphones whose directivity patterns

are of the form  $e(\theta) = A(\cos(\theta - \phi))^n$ , where  $A$  is a constant and  $\phi$  is the angle formed by the microphone's axis and the axis  $x$ . If only pressure microphones are used, then the required gradient responses can be obtained by using the techniques described in Section 3.

In order to show how the gradient microphone techniques can be utilized for realizing higher-order horizontal sound field microphones, three horizontal sound field configurations—two of the second and the other of the third order, are described in detail here. First-order horizontal sound field microphone arrays (e.g., see [23–26]) are not discussed in this paper. The presented microphone topologies are simple, designed with the goal of using the few pressure and first-order gradient microphones for achieving a desired functionality.

### 5.1. Second-order horizontal sound field microphone based on omni microphones

The configuration shown in Fig. 4 can be used for

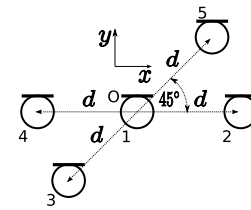


**Fig. 4:** Second-order horizontal sound field microphone array consisting of five pressure microphone elements.

capturing the sound field's circular harmonic coefficients  $a_n(t)$  and  $b_n(t)$  of orders up to two in the point  $O$ . Capturing of these signals can be done as follows:

- The pressure signal  $a_0(t)$ , or the zero-order harmonic, is taken from microphone 1.
- The first-order circular harmonic coefficient  $a_1(t)$ , which corresponds to the circular harmonic  $\cos \theta$ , can be obtained by combining signals from microphones 2 and 4 as follows:

$$a_1(t) = (p_2(t) - p_4(t)) * h_1(t), \quad (18)$$

where  $h_1(t)$  is a filter used for magnitude and phase compensation of the first-order gradient microphone realized from two pressure microphones spaced at the distance  $2d$ .

- The first-order circular harmonic coefficient  $b_1(t)$ , which corresponds to the circular harmonic  $\sin \theta$ , can be obtained by combining signals from microphones 2, 3, 4 and 5. Namely, combining signals from microphones 3 and 5 in the way given in (18) gives the signal

$$c_1(t) = (p_5(t) - p_3(t)) * h_1(t), \quad (19)$$

whose directivity pattern in the working frequency range is of the form  $e_{c_1}(\theta) = \cos(\theta - \frac{\pi}{4})$ . Furthermore, for obtaining the desired response of the form  $\sin \theta$ , signals  $a_1(t)$  and  $c_1(t)$  need to be combined in the following way:

$$b_1(t) = \sqrt{2}c_1(t) - a_1(t). \quad (20)$$

Note that first-order circular harmonic coefficients  $a_1(t)$  and  $b_1(t)$  can be obtained by combining microphone pairs (1, 2) and (1, 5). This approach, described in more detail in [26], would allow increasing the aliasing frequency (due to shorter inter-microphone distance) at a cost of lower SNR at low frequencies and response deviations at high frequencies due to non-coincidence.

- The second-order circular harmonic coefficients  $a_2(t)$  and  $b_2(t)$ , which correspond to the circular harmonics  $\cos 2\theta$  and  $\sin 2\theta$ , can be obtained using the identities

$$\begin{aligned} \cos 2\theta &= 2(\cos \theta)^2 - 1 \\ \sin 2\theta &= 2 \left( \cos \left( \theta - \frac{\pi}{4} \right) \right)^2 - 1, \end{aligned} \quad (21)$$

which relate the circular harmonics  $\cos 2\theta$  and  $\sin 2\theta$ , and directivity patterns of a pressure microphone,  $e_0(\theta) = 1$ , and second-order gradient microphones,  $e_{g_{2,1}}(\theta) = (\cos \theta)^2$  and  $e_{g_{2,2}}(\theta) = (\cos(\theta - \frac{\pi}{4}))^2$ , respectively. The response  $e_0(\theta)$  can be obtained from microphone 1, the response  $e_{g_{2,1}}(\theta)$  by combining microphones 1, 2 and 4, and the response  $e_{g_{2,2}}(\theta)$  by combining microphones 1, 5 and 3. The desired signals are given by

$$\begin{aligned} a_2(t) &= 2 [p_2(t) - 2p_1(t) + p_4(t)] * h_2(t) - p_1(t) \\ b_2(t) &= 2 [p_5(t) - 2p_1(t) + p_3(t)] * h_2(t) - p_1(t), \end{aligned} \quad (22)$$

where  $h_2(t)$  is a filter used for magnitude and phase compensation of the second-order gradient microphone built from three pressure microphones spaced at the distance  $d$ .

## 5.2. Third-order horizontal sound field microphone based on omni microphones

The configuration shown in Fig. 5 can be used for

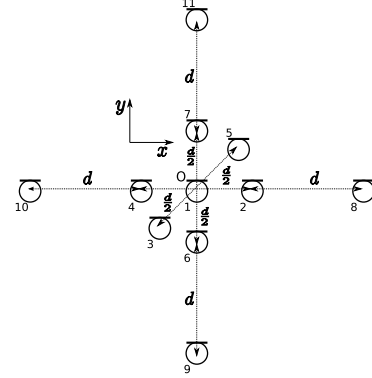


**Fig. 5:** Third-order horizontal sound field microphone configuration with 11 pressure microphone capsules.

capturing the sound field's circular harmonic coefficients  $a_n(t)$  and  $b_n(t)$  of orders up to three in the point  $O$ . Capturing of these signals can be done as follows:

- Circular harmonic coefficients  $a_0(t)$ ,  $a_1(t)$ ,  $a_2(t)$  and  $b_2(t)$  can be captured in the same way as described for the second order horizontal sound field microphone.
- The first-order circular harmonic coefficient  $b_1(t)$  can be captured more simply in this case, by combining the signals from microphones 6 and 7, in the same way as for the signal  $a_1(t)$  in (18):

$$b_1(t) = (p_7(t) - p_6(t)) * h_1(t). \quad (23)$$

- The third-order circular harmonic coefficients  $a_3(t)$  and  $b_3(t)$  can be obtained using the identities

$$\begin{aligned} \cos 3\theta &= 4(\cos \theta)^3 - 3 \cos \theta \\ \sin 3\theta &= 4 \left( \cos \left( \theta + \frac{\pi}{2} \right) \right)^3 + 3 \sin \theta, \end{aligned} \quad (24)$$

which relate the circular harmonics  $\cos 3\theta$  and  $\sin 3\theta$ , and directivity patterns of first-order ( $e_{g_{1,1}}(\theta) = \cos \theta$  and  $e_{g_{1,2}}(\theta) = \sin \theta$ ) and third-order ( $e_{g_{3,1}}(\theta) = (\cos \theta)^3$  and  $e_{g_{3,2}}(\theta) =$

$(\cos(\theta + \frac{\pi}{2}))^3$  gradient microphones. The response  $e_{g_{3,1}}(\theta)$  can be obtained by combining microphones 2, 4, 8 and 10, and the response  $e_{g_{3,2}}(\theta)$  by combining microphones 6, 7, 9 and 11; the ways to obtain responses  $e_{g_{1,1}}(\theta)$  and  $e_{g_{1,2}}(\theta)$  are given in (18) and (23). The desired signals are given by

$$\begin{aligned} a_3(t) &= 4(p_8(t) - 3p_2(t) + 3p_4(t) - p_{10}(t)) * h_3(t) \\ &\quad - 3(p_2(t) - p_4(t)) * h_1(t) \\ b_3(t) &= 4(p_9(t) - 3p_6(t) + 3p_7(t) - p_{11}(t)) * h_3(t) \\ &\quad + 3(p_7(t) - p_6(t)) * h_1(t). \end{aligned} \quad (25)$$

where  $h_3(t)$  is a filter used for magnitude and phase compensation of the third-order gradient microphone built from four pressure microphones spaced at the distance  $d$ .

### 5.3. Second-order horizontal sound field microphone based on omni and bidirectional microphones

Fig. 6 shows a configuration which is similar to the

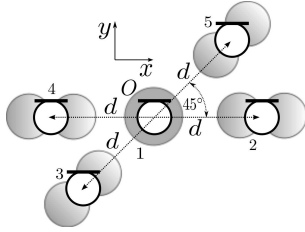


**Fig. 6:** Second-order horizontal sound field microphone array consisting of one omnidirectional and four bidirectional microphone elements.

one shown in Fig. 4, but which uses one pressure microphone capsule in the center  $O$  and four bidirectional (having a figure-of-eight directional response) capsules around it. Capturing the sound field's circular harmonic coefficients  $a_n(t)$  and  $b_n(t)$  of orders up to two can be done similarly:

- The pressure signal  $a_0(t)$ , or the zero-order harmonic, is taken from microphone 1.
- The first-order circular harmonic coefficient  $a_1(t)$  can be obtained by combining signals from microphones 2 and 4 as follows:

$$a_1(t) = (p_2(t) + p_4(t)) * g_1(t), \quad (26)$$

where  $g_1(t)$  is a filter used for magnitude and phase compensation of the first-order gradient response obtained by averaging responses of two bidirectional microphones spaced at the distance  $2d$ .<sup>5</sup>

- The first-order circular harmonic coefficient  $b_1(t)$  can be obtained by combining signals from microphones 2, 3, 4 and 5. Combining signals from microphones 3 and 5 in the way given in (26) gives the signal

$$c_1(t) = (p_5(t) + p_3(t)) * g_1(t), \quad (27)$$

whose directivity pattern is of the form  $e_{c_1}(\theta) = \cos(\theta - \frac{\pi}{4})$ . Further, signals  $a_1(t)$  and  $c_1(t)$  are combined in the following way:

$$b_1(t) = \sqrt{2}c_1(t) - a_1(t). \quad (28)$$

- The second-order circular harmonic coefficients  $a_2(t)$  and  $b_2(t)$  can be obtained using the identities (21). The response  $e_0(\theta)$  is obtained from microphone 1, the response  $e_{g_{2,1}}(\theta)$  by combining microphones 2 and 4, and the response  $e_{g_{2,2}}(\theta)$  by combining microphones 5 and 3. The desired signals are given by

$$\begin{aligned} a_2(t) &= 2[p_2(t) - p_4(t)] * h_2(t) - p_1(t) \\ b_2(t) &= 2[p_5(t) - p_3(t)] * h_2(t) - p_1(t), \end{aligned} \quad (29)$$

where  $g_2(t)$  is a filter used for magnitude and phase compensation of the second-order gradient microphone built from two bidirectional microphones spaced at the distance  $2d$ .

The second-order configuration from Fig. 6 provides better signal-to-noise ratio than the one shown in Fig. 4, even though they both use the same number of microphone capsules.

## 6. SIMULATIONS

In order to assess the practical characteristics of the microphone arrays proposed in Section 5, the following simulations were performed:

- Simulation of the array's response at different frequencies for different angles of sound arrival.

<sup>5</sup>The response of the compensation filter  $g_1(t)$  is low-pass, unlike the high-pass compensation filters for differential microphones.



- Simulation of the array's self-noise sensitivity, showing how much the uncorrelated internal capsule noise gets amplified when forming different directional responses.

### 6.1. Simulation setup

The simulations tested the second-order horizontal sound field microphone, shown in Fig. 4 and described in Section 5.1. The tested microphone consisted of five virtual pressure microphones located in the free field, and the used inter-microphone spacing was  $d = 2$  cm. The microphone array's response was computed using simulated far-field (or plane-wave) sound sources having different directions  $\theta$  and angular frequencies  $\omega$ . Signals at each simulated microphone were computed by introducing a delay

$$t_d = \frac{\mathbf{k} \cdot \mathbf{r}}{\omega} \quad (30)$$

to the source signal, where  $\mathbf{r}$  is the microphone position vector,  $\mathbf{k}$  the wave vector, and  $\omega$  the angular frequency.

Microphone signals were sampled with the sampling frequency  $f_s = 44.1$  kHz. The processing, including generation of different responses and their subsequent frequency equalization, and the compensation filter design were done in the short-time Fourier transform (STFT) domain [27, 28].

The compensation filters  $h_1[n]$  and  $h_2[n]$ , used for the equalization of the frequency characteristics of the first- and second-order sound pressure gradient responses, have been designed in the following way:

- At low frequencies, where the gains of the obtained gradient responses are very low, the desired signals are highly attenuated and would therefore need very high compensation gains. In order to avoid using large gains and amplifying the internal noise excessively, the compensation filters' gains were bounded to a predefined maximum value of 35 dB.

Note that at low frequencies the gradient microphone effectively reduces the signal-to-noise ratio (SNR) of the used pressure microphones, such that the maximum low-frequency gain has to be carefully chosen, depending on the SNR of the used pressure microphone capsules. Since

SNR of pressure capsules is commonly around 60 dB, the maximum gain of 35 dB was chosen in order to avoid over-amplifying the noise at frequencies where the SNR is lower than 25 dB.

- At frequencies where the magnitude frequency characteristics of the obtained gradient responses are approximately linear, up to the frequency  $f_m = \frac{c}{2d}$  where the magnitude characteristics reach their first maximums, the compensation filters are equal to the inverse of the frequency characteristics given in (8), for the angle  $\theta = 0$ .
- Above the frequency  $f_m$ , the compensation filters' magnitude responses are bounded to their values at the frequency  $f_m$ , since at higher frequency, the frequency-characteristics become noticeably angle-dependent due to spatial aliasing.

The frequency responses of the filters  $h_1[n]$  and  $h_2[n]$  can be summarized in the following expression:

$$H_i(e^{j\omega}) = \begin{cases} \min(G, (2j)^{-i} (\sin(\pi\omega f_s d))^{-i}) & \omega \leq \omega_m \\ (2j)^{-i} (\sin(\pi\omega f_s d))^{-i} & \omega > \omega_m \end{cases} \quad (31)$$

where  $G = 10^{1.75}$  is a constant maximum gain,  $\omega_m$  is the maximum normalized angular frequency corresponding to  $f_m$  ( $\omega_m = \frac{2\pi f_m}{f_s}$ ), and  $f_s$  is the sampling frequency. The frequency responses  $H_1(e^{j\omega})$  and  $H_2(e^{j\omega})$  are shown in Fig. 7.

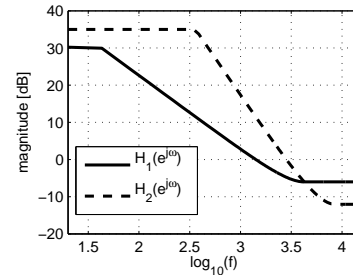


**Fig. 7:** Magnitude frequency responses of the first- and second-order gradient compensation filters  $h_1[n]$  and  $h_2[n]$  used in the simulation.

### 6.2. Results

Fig. 8 shows the simulated array's first- ( $a_1[n]$  and  $b_1[n]$ ) and second-order ( $a_2[n]$  and  $b_2[n]$ ) circular harmonic responses at different frequencies.

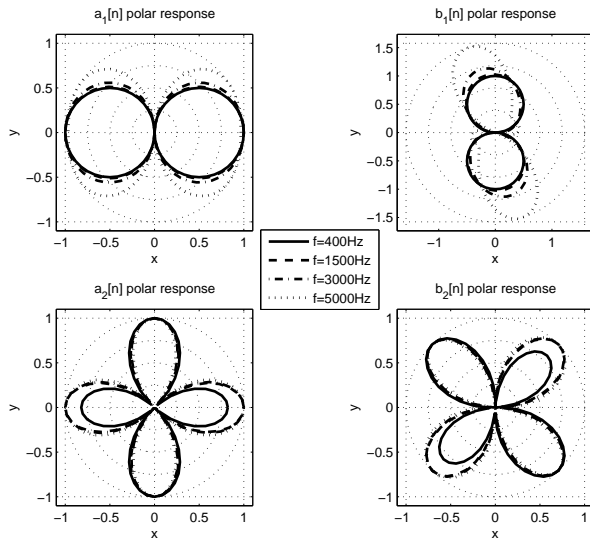


**Fig. 8:** Polar characteristics at different frequencies of signals  $a_1[n]$ ,  $b_1[n]$ ,  $a_2[n]$  and  $b_2[n]$  obtained from the simulation of the second-order horizontal sound field microphone configuration shown in Fig. 4.

The first-order circular harmonic response  $a_1[n]$  has a desired polar characteristic up to the frequency of around 3 kHz. The aliasing problems start to be more noticeable above 3 kHz, which is reflected in the polar characteristics of  $a_1[n]$  at 3 kHz and 5 kHz.

The other first-order circular harmonic response,  $b_1[n]$ , experiences higher deviations at high frequencies. The problem stems from computing the signal  $b_1[n]$  from two microphone pairs—(2, 4) and (3, 5)—with different orientations and non-linear responses, given in (8). Also, the polar characteristic of  $b_1[n]$ , besides the deviations in shape, has the maximum response which exceeds unity at higher frequencies, but the maximum gain can be normalized by a post-filter.

The cause of aliasing at a relatively low frequency of around 3 kHz for responses  $a_1[n]$  and  $b_1[n]$  relates to a larger inter-microphone distance ( $2d = 4$  cm) between microphone pairs (2, 4) and (3, 5).

Since the microphones used for computing responses  $a_2[n]$  and  $b_2[n]$  are more closely spaced (at distance  $d = 2$  cm), these two responses exhibit less aliasing problems at high frequencies. However, their low-frequency polar characteristics deviate (lobes have

different magnitudes) as a consequence of using compensation filter  $H_2(e^{j\omega})$  which is bounded at low frequencies.

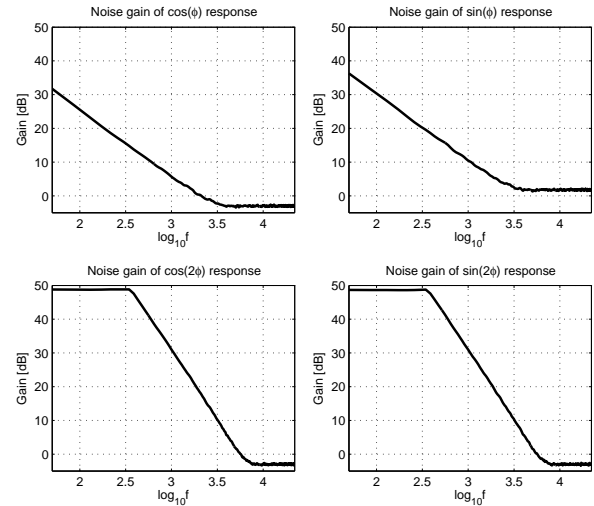


**Fig. 9:** Uncorrelated noise gain frequency characteristics of different circular harmonic coefficients of the second-order horizontal sound field microphone configuration shown in Fig. 4.

Fig. 9 shows the sensitivity of the obtained circular harmonic responses to uncorrelated Gaussian self-noise of unit variance. The simulation consisted of feeding each virtual pressure microphone in the array with a Gaussian white noise of unit variance and comparing the energy at microphones' inputs with the energy of the processed output signals at different frequencies.

Signal  $a_1[n]$  is the least sensitive to noise, since it is obtained by combining only two pressure microphone signals (i.e., two uncorrelated noise sources); signal  $b_1[n]$ , involving the combination of four microphones, has the noise gain which is approximately 6 dB higher than the noise gain of  $a_1[n]$ .

Signals  $a_2[n]$  and  $b_2[n]$  have higher noise gain at low frequencies than the first-order circular harmonic response  $a_1[n]$ , and it is caused by the use of more microphone elements. In addition, their noise gain decays faster, following the 6 dB/oct low-frequency characteristic of the second-order gradient compensation filter. The high noise gain at lowest frequencies can be reduced by setting a lower maximum

gain for the gradient response compensation filter  $h_2[n]$ , or by increasing the inter-microphone distance  $d$ . However, increasing  $d$  decreases the aliasing frequency.

## 7. CONCLUSIONS

A relation was established between the horizontal sound field analysis by its plane wave decomposition (commonly used in surround sound system analysis), the horizontal sound field description by its circular harmonic coefficients in a single point, and the horizontal sound field's gradients measured in that point.

Subsequently, it was shown how with the help of the aforementioned relation, horizontal sound field microphones can be built using coincident gradient microphones.

Practically, higher-order gradient-based horizontal sound field microphones can be built using an array of a few pressure or first-order gradient microphone capsules. This paper proposed horizontal sound field microphones of orders two and three that use five and eleven microphone elements, respectively, and their feasibility has been confirmed with simulation experiments.

## 8. REFERENCES

- [1] Harry F. Olson, "Gradient microphones," *J. Acoust. Soc. Am.*, vol. 17, no. 3, pp. 192–198, January 1946.
- [2] Harry F. Olson, "Directional microphones," *Journal of the Audio Engineering Society*, vol. 15, no. 4, pp. 420–430, October 1967.
- [3] G. M. Sessler and J. E. West, "Directional transducers," *IEEE Transactions on Audio and Electroacoustics*, vol. AU-19, no. 1, pp. 19–23, March 1971.
- [4] M. A. Poletti, "The design of encoding functions for stereophonic and polyphonic sound systems," *Journal of the audio Engineering Society*, vol. 44, no. 11, pp. 948–963, November 1996.
- [5] A. Blumlein, "Improvements in and relating to sound transmission, sound recording and sound reproduction systems," *British Patent Specification 394325*, 1931, Reprinted in *Stereophonic Techniques*, Aud. Eng. Soc., New York, 1986.
- [6] M. A. Gerzon, "Periphony: Width-Height Sound Reproduction," *J. Aud. Eng. Soc.*, vol. 21, no. 1, pp. 2–10, Jan. 1973.
- [7] M. A. Gerzon, "The design of precisely coincident microphone arrays for stereo and surround sound," in *Preprint 50th Conv. Aud. Eng. Soc.*, Mar. 1975.
- [8] M. A. Gerzon, "Practical periphony: The reproduction of full-sphere sound," in *Preprint 65th Conv. Aud. Eng. Soc.*, Feb. 1980.
- [9] K. Farrar, "Soundfield microphone," *Wireless World*, pp. 48–50, Oct. 1979.
- [10] Jeffery S. Bamford and John Vanderkooy, "Ambisonic sound for us," in *Preprint 99th Conv. Aud. Eng. Soc.*, Oct 6–9 1995.
- [11] J. Daniel, *Acoustic field representation, application to the transmission and the reproduction of complex sound environments in a multimedia context*, Ph.D. thesis, Université Paris 6, 2000, in French.
- [12] M. A. Poletti, "A unified theory of horizontal holographic sound systems," *Journal of the audio Engineering Society*, vol. 48, no. 12, pp. 1155–1182, December 2000.
- [13] Thushara D. Abhayapala and Darren B. Ward, "Theory and design of high order sound field microphones using spherical microphone array," in *Proc. IEEE ICASSP-02*, May 2002, pp. 1949–1952.
- [14] Jens Meyer and Tony Agnello, "Spherical microphone array for spatial sound recording," in *Preprint 115th Conv. Aud. Eng. Soc.*, Oct 2003.
- [15] Jens Meyer and Gary Elko, "A highly scalable spherical microphone array based on an orthonormal decomposition of the soundfield," in *Proc. IEEE ICASSP-02*, May 2002, pp. 1781–1784.

- [16] Boaz Rafaely, "Analysis and design of spherical microphone arrays," *IEEE Transactions on Speech and Audio Processing*, vol. 13, no. 1, pp. 135–143, Jan 2005.
- [17] Earl G. Williams, *Fourier acoustics: sound radiation and nearfield acoustical holography*, Academic Press, London, 1999.
- [18] Philip S. Cotterell, *On the theory of the second-order Soundfield microphone*, Ph.D. thesis, The University of Reading, 2002.
- [19] Gary W. Elko, "Superdirectional microphone arrays," in *Acoustic signal processing for telecommunication*, pp. 181–238. Kluwer Academic Publishers, 2000.
- [20] Harry F. Olson, "Gradient loudspeakers," *Journal of the Audio Engineering Society*, vol. 21, no. 2, pp. 86–93, Mar 1973.
- [21] Gary W. Elko, "Microphone array systems for hands-free telecommunication," *Speech communication*, vol. 20, no. 3–4, pp. 229–240, December 1996.
- [22] M. Kolundžija, C. Faller, and M. Vetterli, "Spatio-Temporal Gradient Analysis of Differential Microphone Arrays," in *Preprint 126th Conv. Aud. Eng. Soc.*, May 2009.
- [23] Gary W. Elko, "Steerable and variable first-order differential microphone array," *US Patent Number: 6,041,127*, March 2000.
- [24] Juha Merimaa, "Applications of a 3-D microphone array," in *Preprint 112th Conv. Aud. Eng. Soc.*, May 10–13 2002.
- [25] V. Pulkki and C. Faller, "Directional audio coding: filterbank and STFT-based design," in *AES 120th Convention*, 2006.
- [26] M. Kolundžija, "Microphone processing for sound field measurement," M.S. thesis, EPFL, 2007.
- [27] Jont B. Allen, "Short term spectral analysis, synthesis, and modification by discrete Fourier transform," *IEEE Trans. Acoust., Speech, Signal Processing*, vol. ASSP-25, no. 3, pp. 235–238, Jun 1977.
- [28] Jont B. Allen and Lawrence R. Rabiner, "A unified approach to short-time Fourier analysis and synthesis," *Proceedings of the IEEE*, vol. 65, no. 11, pp. 1558–1564, Nov 1977.